Acta Mech Sin (2007) 23:145–148
DOI 10.1007/s10409-007-0060-y

RESEARCH PAPER

Kinetic assessment of measured mass flow rates and streamwise pressure distributions in microchannel gas flows

Jing Fan · Chong Xie · Jianzheng Jiang

Received: 19 May 2006 / Revised: 20 November 2006 / Accepted: 5 December 2006 / Published online: 17 March 2007

Abstract Measured mass flow rates and streamwise pressure distributions of gas flowing through microchannels were reported by many researchers. Assessment of these data is crucial before they are used in the examination of slip models and numerical schemes, and in the design of microchannel elements in various MEMS devices. On the basis of kinetic solutions of the mass flow rates and pressure distributions in microchannel gas flows, the measured data available are properly normalized and then are compared with each other. The 69 normalized data of measured pressure distributions are in excellent agreement, and 67 of them are within 1 ± 0.05. The normalized data of mass flow-rates ranging between 0.95 and 1 agree well with each other as the inlet Knudsen number $Kn_i < 0.02$, but they scatter between 0.85 and 1.15 as $Kn_i > 0.02$ with, to some extent, a very interesting bifurcation trend.

Keywords Microchannel · Measured data · Kinetic assessment

1 Introduction

It is well known that from the classical hydrodynamics [1] the streamwise pressure distribution for a low subsonic gas flow through a long channel with two parallel walls is linear and the mass flow rate may be expressed as

$$M_{N-S} = -\frac{\rho h^3 w}{12\mu}\frac{\mathrm{d}p}{\mathrm{d}x}, \tag{1}$$

where h and w are the channel height and width, respectively, ρ the density, μ the gas viscosity, and the negative pressure gradient $\mathrm{d}p/\mathrm{d}x$ is constant.

According to the kinetic theory [2], there is a condition for the non-slip Navier–Stokes solution (1) to be accurate. This condition is that the Knudsen number (Kn), a ratio of the molecular mean free path λ to h, is smaller than 0.01. The mean free path is usually very small, for example, at the standard condition (101,325 Pa and 273 K), about 0.05 μm for nitrogen and argon, and 0.16 μm for helium. The channel heights in common applications are much larger than the mean free path, and therefore the linear pressure distribution and mass flow rate (1) are accurate for those cases.

For microchannels greatly interested in recent years, however, the values of h become comparable with the mean free path. The microchannel dimensions used in experiments [3–9] were order of one micron high, several tens microns wide, and several thousands microns long. The corresponding Knudsen number is approximately 0.05 for nitrogen and argon, and 0.16 for helium at the standard conditions [3–9], and 2.5 for helium at a low pressure of 6,500 Pa [7]. To evaluate the microscale effects elaborate measurements were carried out. The measured pressure distributions in the streamwise direction were nonlinear [3,5,9], and the measured mass flow rate [4–9] deviated significantly from the solution (1). Many theoretical studies have been performed to understand the differences between the experimental and classical results, including the study of various slip boundary conditions [5–12] used to extend the continuum approach to the slip regime ($0.01 < Kn < 0.1$),

The project supported by the National Natural Science Foundation of China (90205024, 10621202 and 10425211).

J. Fan (✉) · C. Xie · J. Jiang
Institute of Mechanics, Chinese Academy of Sciences, Beijing 100080, China
e-mail: jfan@imech.ac.cn

and the development of kinetic schemes [13–15] that are more physically appropriate for microscale gas flows.

The present article provides an analytically kinetic description of microchannel gas flows that is suitable to the entire Knudsen regime, and assesses different sets of measured data given by many researcher [3–9]. In light of the different experimental conditions and measurement techniques, the assessment is crucial for the measured data used as benchmark to test various slip models and numerical schemes. Moreover, as a basic element of MEMS, the reliable data and analytical relations of various microchannel-flow quantities based on the careful examination and the assessment are essential to design and optimization of MEMS devices.

2 Kinetic analysis of microchannel gas flows

Because the width-to-height ratios of experimental microchannels are greater than 30, the spanwise effects due to the lateral walls are negligible [16]. In addition, the experimental conditions are low subsonic ($Ma \ll 1$) and without external heating, the isothermal assumption is valid therefore. This simplifies the theoretical analysis considerately, and the flow at a cross section of the microchannels may be localized as the Poiseuille flow.

The mass flow rate for Poiseuille flows over the entire Knudsen regime from continuum to free molecular may be written as [17–20]

$$M_k = \phi(Kn) \cdot M_{N-S}, \tag{2}$$

where $\phi(Kn)$ reflects the local deviation from the non-slip solution (1) owing to the microscale effect. The relation of ϕ to Kn may be numerically obtained through kinetic approaches [17–20]. A tabulated database of $\phi(Kn)$ calculated by using the linearized Boltzmann equation was provided in Ref. [19], and for a diffuse reflection boundary condition a fitting formula was available [21]

$$\phi(Kn) = 1 + 6\alpha Kn + \frac{12}{\pi} Kn \ln(1 + \beta Kn), \tag{3}$$

with $\alpha = 1.318\,889$, $\beta = 0.387\,361$.

The mass flow rate conservation along a microchannel requires

$$\frac{\mathrm{d}M_k}{\mathrm{d}x} = 0. \tag{4}$$

Substituting Eqs. (2) and (3) into Eq. (4) yields

$$\frac{\mathrm{d}}{\mathrm{d}x}\left\{\left[1 + 6\alpha Kn + \frac{12}{\pi} Kn \ln(1 + \beta Kn)\right] p \frac{\mathrm{d}p}{\mathrm{d}x}\right\} = 0, \tag{5}$$

where the state equation of ideal gases $p = \rho RT$ is employed, and the constant term $-2h^3/(3\mu RT)$ is eliminated.

The kinetic kernel (3) is valid over the entire flow regime, so is Eq. (5). This equation may be regarded as a special case of the generalized Reynolds equation with a bearing number $\Lambda = 0$, as noted by Shen [22]. The generalized Reynolds equation itself was firstly derived by Fukui and Kaneko [23], and it works quite well for air slider bearings in magnetic recording applications where the read-write head has a minimum separation from the disk of order 100 nm or less.

Although Eq. (5) may be numerically solved as shown in Ref. [21], it is always preferable to have an analytical solution that may reveal the physical characteristics more directly and clearly. For hard-sphere molecules, the mean free path $\lambda = kT/\sqrt{2}\sigma_T p$, where the collision cross section σ_T is constant. Thus, the Knudsen number along a microchannel at the isothermal condition may be written as

$$Kn \equiv \frac{\lambda}{h} = \frac{\lambda_\mathrm{o}}{h} \times \frac{\lambda}{\lambda_\mathrm{o}} = Kn_\mathrm{o} \times \frac{p_\mathrm{o}}{p} = \frac{Kn_\mathrm{o}}{P}, \tag{6}$$

where $P = p/p_\mathrm{o}$, and the subscript "o" denotes the outlet.

If we substitute Eq. (6) into Eq. (5), and integrate Eq. (5) from $x = 0$ forward, we obtain

$$\frac{\mathrm{d}P}{\mathrm{d}X} = \frac{C}{P \cdot \phi(Kn)}, \tag{7}$$

and

$$\begin{aligned}&\frac{1}{2}(P^2 - \vartheta^2) + 6\alpha Kn_\mathrm{o}(P - \vartheta)\\ &+ \frac{12Kn_\mathrm{o}}{\pi}\left[P \ln\left(1 + \frac{\beta Kn_\mathrm{o}}{P}\right) - \vartheta \ln\left(1 + \frac{\beta Kn_\mathrm{o}}{\vartheta}\right)\right.\\ &\left.+ \beta Kn_\mathrm{o} \ln\left(\frac{P + \beta Kn}{\vartheta + \beta Kn_\mathrm{o}}\right)\right] = CX,\end{aligned} \tag{8}$$

where $\vartheta \equiv p_i/p_\mathrm{o}$, $X = x/L$, and L is the channel length.

The constant C in Eq. (8) is determined by using the outlet boundary condition ($X = 1, P = 1$)

$$\begin{aligned}C = &\frac{1}{2}(1 - \vartheta^2) + 6\alpha Kn_\mathrm{o}(1 - \vartheta)\\ &\times \frac{12Kn_\mathrm{o}}{\pi}\left[\ln(1 + \beta Kn_\mathrm{o}) - \vartheta \ln\left(1 + \frac{\beta Kn_\mathrm{o}}{\vartheta}\right)\right.\\ &\left.+ \beta Kn_\mathrm{o} \ln\left(\frac{1 + \beta Kn_\mathrm{o}}{\vartheta + \beta Kn_\mathrm{o}}\right)\right].\end{aligned} \tag{9}$$

Substitution of Eqs. (1) and (7) into Eq. (2) yields

$$M_k = \phi(Kn)\cdot M_{N-S} = -\phi(Kn)\times\frac{\rho h^3 w}{12\mu}\times\frac{Cp_0^2}{\phi(Kn)pL} = -\frac{Ch^3 w p_0^2}{12\mu RTL}, \tag{10}$$

or

$$M_k = -\frac{h^3 w p_0^2}{12\mu RTL}\Big\{\frac{1}{2}(1-\vartheta^2)+6\alpha Kn_o(1-\vartheta) + \frac{12Kn_o}{\pi}\Big[\ln(1+\beta Kn_o)-\vartheta\ln\Big(1+\frac{\beta Kn_o}{\vartheta}\Big) + \beta Kn_o\ln\Big(\frac{1+\beta Kn_o}{\vartheta+\beta Kn_o}\Big)\Big]\Big\}. \tag{11}$$

Note that the first two terms on the right-hand-side of Eq. (11) are the slip Navier–Stokes solution given by Arkilic et al. (see (2.3) in Ref. [8]).

For other surface boundary conditions or geometric cross sections, e.g. with a momentum accommodation coefficient $\sigma < 1$ or a circular cross section, the present method is still valid but the fitting formula (3) needs to be modified on the basis of a database obtained from the corresponding boundary condition or geometric cross section.

3 Kinetic assessment of measured data

Equation (11) holds in the whole Knudsen regime that clearly reveals the relation of the mass flow rate to the various parameters. It may be used to analyze and understand microchannel flows. For instance, in a recent experiment of low-speed gas flow in a long constant-area microchannel carried out by Yao et al. [24], a so called sub-choking phenomenon was observed, namely the mass flow rate in the microchannel changed little as the inlet-to-outlet pressure ratio reached a critical value. This is easily understood from Eq. (11). At their experimental conditions, the outlet Knudsen number was about 0.05 or less. Therefore, as the inlet-to-outlet pressure ratio ϑ increases and reaches a value much larger than 1, the first term on the right-hand-side of Eq. (11) becomes dominate, and M_k may be simplified as

$$M_k \approx -\frac{h^3 w p_0^2}{12\mu RTL}\times\frac{1}{2}(1-\vartheta^2) \cong \frac{h^3 w p_i^2}{24\mu RTL}. \tag{12}$$

Equation (12) indicates that the mass flow rate in this situation is approximately independent on ϑ or more exactly the outlet pressure. Moreover, the kinetic solution (11) demonstrates that the critical value of ϑ beyond which the sub-choking phenomenon takes place depends upon Kn_o rather than the surface-to-volume ratio claimed in Ref. [24].

A typical method to examine and assess measured data is to normalize them firstly, then compare the normalized data with each other and examine whether they are consistent or not. The proper normalization is critical to the successful examination and assessment, and therefore the normalized factor must be chosen correctly. Because of the similarity parameter difference between the continuum and rarefied gas flows, the normalized factors of mass flow rate and pressure distribution in microchannels have to employ the kinetic solutions (11) and (8) rather than (1) and the linear solution.

Figure 1 compares experimental pressure distributions given by Pong et al. [3], Shih et al. [5], and Zohar et al. [9]. The four series of experiments have the same outlet pressure of 1 atm, but the test gases, inlet pressures, and channel heights and lengths are different (Table 1). All the pressure data p_{exp} are normalized by the corresponding kinetic solution (8). The comparison is very satisfactory: the total number of measured data is 69 and 67 of them have pressure values of p_{exp}/p_k

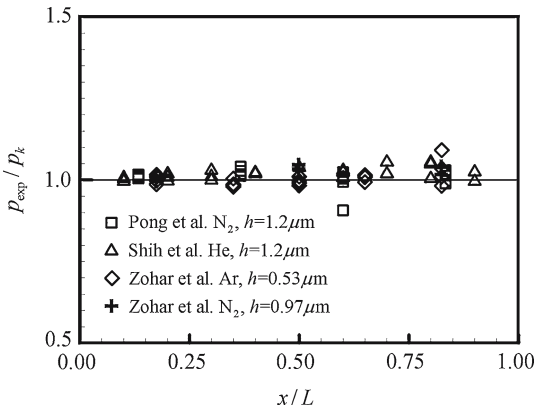

Fig. 1 Comparison of normalized measured data of the streamwise pressure distributions along microchannels

Table 1 Experimental conditions for microchannel pressure measurements

Case	Author	Gas	Height/ μm	Width/ μm	Length/ μm
A1-A5[a]	Pong et al. [3]	N_2	1.2	40	3,000
B1-B3[b]	Shih et al. [5]	He	1.2	40	4,000
C1-C3[c]	Zohar et al. [9]	N_2	0.53	40	4,000
D1-D4[d]	Zohar et al. [9]	Ar	0.97	40	4,000

[a] Values of the inlet pressure P_i for A1-A5 are 25, 20, 15, 10 and 5 psig, respectively
[b] Values of P_i for B1-B3: 19, 13.6 and 8.7 psig
[c] Approximate values of P_i for C1-C3: 2.1, 2.8 and 3.4 atm
[d] Approximate values of P_i for D1-D4: 1.9, 2.6, 3.3 and 4 atm

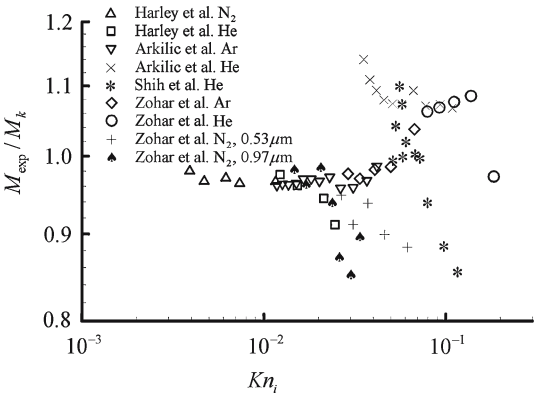

Fig. 2 Comparison of normalized measured data of mass flow rates through microchannels versus the inlet Knudsen number

Table 2 Experimental conditions for microchannel mass-flow-rate measurements

Author	Gas	Height/μm	Width/μm	Length/μm
Harley et al. [4]	N_2, He	0.51	97	10,900
Shih et al. [5]	He	1.2	40	4,000
Arkilic et al. [6,8]	He, Ar	1.33	52.3	7,490
Zohar et al. [9]	He, Ar	0.53	40	4,000
Zohar et al. [9]	N_2	0.53, 0.97	40	4,000

ranging between 0.95 and 1.05. The two measured data beyond the range appear in case A4 ($x = 1,800\,\mu$m, $p_{\rm exp}/p_k = 0.91$), and case D4 ($x = 3,300\,\mu$m, $p_{\rm exp}/p_k = 1.09$). Note that the pressure data of helium are in excellent agreement with those of nitrogen and argon. The pressure distribution (8) in excellent agreement with the experiments is recommended for the design of a microchannel element in MEMS devices.

Figure 2 compares measured mass flow rates given by Harley et al. [4], Shih et al. [5], Arkilic et al. [6,8], and Zohar et al. [9]. The experimental conditions are given in Table 2. The measured data are all normalized by the corresponding kinetic solution (10). As $Kn_i < 0.02$, the normalized measured data are in excellent agreement with general range between 0.95 and 1. As $Kn_i > 0.02$, the distribution range of the normalized data is approximately 1 ± 0.15 that is obviously larger in comparison with the situation of $Kn_i < 0.02$. A possible reason is that for the nanoliter flow rates concerned here, the mass flow rates decreases as the inlet Knudsen number increases, and accurate measurement of flow rate becomes more difficult.

References

1. Batchelor, G.K.: An Introduction to Fluid Dynamics. Cambridge University Press, Cambridge (1973)
2. Chapman, S., Cowling, T.G.: The Mathematical Theory of Non-Uniform Gases. Cambridge University Press, Cambridge (1970)
3. Pong, K.C., Ho, C.M., Liu, J.Q., Tai, Y.C.: Non-linear pressure distribution in uniform micro-channels. ASME-FED **197**, 51–56 (1994)
4. Harley, J.C., Huang, Y., Bau, H., Zemel, J.N.: Gas flow in micro-channels. J. Fluid Mech. **284**, 257–274 (1995)
5. Shih, J.C., Ho, C.M., Liu, J.Q., Tai, Y.C.: Monatomic and polyatomic gas flow through uniform microchannels. ASME-DSC **59**, 197–203 (1996)
6. Arkilic, E.B., Schmidt, M.A., Breuer, K.S.: Measurement of the TMAC in silicon microchannels. In: Shen C. (ed) Rarefied Gas Dynamics, pp. 983–988. Peking University Press, Beijing (1997)
7. Arkilic, E.B.: Measurement of the mass flow and tangential momentum accommodation coefficient in silicon microchannels. Ph.D. thesis, FDRL TR 97-1, MIT (1997)
8. Arkilic, E.B., Breuer, K.S., Schmidt, M.A.: Mass flow and tangential momentum accommodation in silicon micromachined channels. J. Fluid Mech. **437**, 29–43 (2001)
9. Zohar, Y., Lee, S.Y.K., Lee, W.Y., Jiang, L., Tong, P.: Subsonic gas flow in a straight and uniform microchannel. J. Fluid Mech. **472**, 125–151 (2002)
10. Beskok, A., Karniadakis, G.: Rarefaction and compressibility effects in gas microflows. J. Fluids Eng. **11**, 448–456 (1996)
11. Maurer, J., Tabeling, P., Joseph, P., Willaime, H.: Second-order slip laws in microchannels for helium and nitrogen. Phys. Fluids **15**, 2613–2621 (2003)
12. Myong, R.S.: Gaseous slip models based on the Langmuir absorption isotheme. Phys. Fluids **16**, 104–117 (2004)
13. Xie, C., Fan, J., Shen, C.: Statistical simulation of rarefied gas flows in micro-channels. In: Ketsdever, A.D., Muntz, E.P. (eds.) Rarefied Gas Dynamics, pp. 800–807. AIP, New York (2003)
14. Shen, C., Fan, J., Xie, C.: Statistical simulation of rarefied gas flows in micro-channels. J. Comput. Phys. **189**, 512–526 (2003)
15. Xu, K., Li, Z.H.: Microchannel flows in slip flow regime: BGK-Burnett solutions. J. Fluid Mech. **513**, 87–110 (2004)
16. Sharipov, F.: Rarefied gas flows through a long rectangular channel. J. Vac. Sci. Technol. A **17**, 3062–3066 (1999)
17. Cercigani, C., Daneri, A.: Flow of a rarefied gas between two parallel plates. J. Appl. Phys. **34**, 3509–3513 (1963)
18. Ohwada, T., Sone, Y., Aoki, K.: Numerical analysis of the Poiseuille flow and thermal transpiration flows between two parallel plates on the basis of the linearized Boltzmann equation for hard-sphere molecules. Phys. Fluids **1**, 2042–2049 (1989)
19. Fukui, S., Kaneko, R.: A database for interpolation of Poiseuille flow rates for high Knudsen number lubrication problem. J. Tribol. **112**, 78–83 (1990)
20. Fan, J., Shen, C.: Statistical simulation of low-speed rarefied gas. J. Comput. Phys. **167**, 393–412 (2001)
21. Alexander, F.J., Garcia, A.L., Alder, B.J.: Direct simulation Monte Carlo for thin-film bearings. Phys. Fluids **6**, 3854–3860 (1994)
22. Shen, C.: Use of the degenerated Reynolds equation in solving the microchannel gas flow problem. Phys. Fluids **17**, 046101 (2005)
23. Fukui, S., Kaneko, R.: Analysis of ultrathin gas film lubrication based on linearized Boltzmann equation: First report derivation of a generalized lubrication equation including thermal creep flow. J. Tribol. **110**, 253–262 (1988)
24. Yao, Z.H., He, F., Ding, Y.T., Shen, M.Y., Wang, X.F.: Low-speed gas flow subchoking phenomenon in a long constant area microchannel. AIAA J. **42**, 1517–1521 (2004)